

Magnitude of inverse Faraday effect induced by circularly polarized laser pulses

A. Kundu and S. Zhang

Department of Physics, University of Arizona, Tucson AZ 85721.

(Dated: December 3, 2024)

Abstract

A leading explanation of experimentally observed magnetization switching in magnetic materials by using ultrafast circularly polarized laser pulses has been attributed to the inverse Faraday effect in which an optically induced non-equilibrium orbital momentum generates an effective magnetic field via spin-orbit coupling for magnetization rotation and switching. We critically examine this scenario by explicitly calculating the magnitude of the induced orbital moment for generic itinerant bands and found that the induced momentum is at least two to three orders of magnitude too small to be responsible for the observed switching phenomena.

I. INTRODUCTION

Laser-induced ultrafast magnetization switching have been experimentally demonstrated in a number of rare earth and transition metal compounds or multilayers [1–4]. The essential role of the laser is to heat the magnetic sample to a high temperature close to the Curie temperature in less than picosecond time scale and the subsequent cooling reorients the magnetization in the direction opposite to the initial one. When the laser field is unpolarized or linearly polarized, laser heating would reduce the magnitude of the magnetization known as demagnetization process [5], but there is no external torque to rotate the magnetization away from its initial direction. The observed magnetization switching [6] by laser heating without polarization must involve spatial/time reversal symmetry breaking processes such as highly non-uniform magnetization distributions. Model calculations have also indicated that the initial non-collinear canting angles between Fe and Gd moments in the ferrimagnetic compound FeGd are necessary to break the spatial inversion symmetry so that the internal exchange interaction upon the heating and cooling would favor one direction of the magnetization than the other [7, 8]. Thus, the heat induced switching is unlikely an intrinsic effect, namely, it depends on details of the inhomogeneous distribution of the magnetic configurations and it is doubtful that the controlled switching at nano-scales with nearly-single domain particles can be achieved.

Recently, all-optical helicity-dependent magnetization switching has been observed [4, 9] in which the switching occurs only for the laser pulse with a definitive helicity: a right-circularly polarized light (PL) is able to switch the magnetization from up to down while the left-circularly PL can switch it back, and the linearly-polarized or unpolarized lights do not do either switching. The circularly PL itself carries the angular momentum, the (direct or indirect) interaction between the light and spins may facilitate the magnetization switching. The inverse Faraday effect (IFE), which is synonym with the laser induced non-equilibrium electron orbital moment, has been proposed as a leading mechanism [10, 11]. If the laser induced orbital moment is sufficiently large and the spin-orbit coupling is sufficiently strong, the magnetization can be switched to the direction of the induced orbital moment that is determined by the polarization of the light. Indeed, theoretical models have already been developed for explaining the laser-induced magnetization switching by the IFE [12–14]. A formulation in which the induced moment is expressed in terms of exact band states have also

been constructed [15]. However, these calculations do not quantitatively address whether the IFE alone is able to account for the experimental results.

In this paper, we calculate the laser induced orbital moments by considering several different models. The essential goal is to estimate the magnitude of the orbital momentum for a given value of the laser intensity used in the switching experiments. In Sec. II, we discuss the minimum induced orbital moment required for switching and give a rough estimate based on the free electron model. In Sec. III, we present the IFE for arbitrary itinerant bands. The results are then applied to a tight-binding band. In Sec. IV, we estimate the induced orbital moments with experimental parameters. In Sec. V we discuss possible mechanisms for observed magnetization switching and we conclude in Sec. VI.

II. CONDITIONS OF MAGNETIZATION SWITCHING BY THE IFE

The idea of the magnetization switching by the IFE is that the induced non-equilibrium orbital moment generates an effective field on the spin via spin-orbit coupling $H = \xi \mathbf{s} \cdot \delta \mathbf{L}$ where ξ is the spin-orbit coupling strength, $\delta \mathbf{L}$ is the induced orbital moment. To switch the spin within the laser pulse duration t_p , which is typically less than a pico-second, the effective field $H_{eff} = \xi \delta \mathbf{L}$ must be at least of the order of $1/(\gamma t_p) > 100$ (T) where γ is the gyromagnetic ratio. With this simple reasoning, the IFE would require an induced orbital momentum at least on the order of $\delta L = 0.1\hbar$ per magnetic ion if we take the spin-orbit coupling strength of the order of 0.1 eV. To see whether the experimental parameters could generate such magnitude of the orbital momentum, we shall make two rough estimates below.

First, we estimate the total angular momentum of the circularly polarized light received by the magnetic film during laser radiation,

$$\delta \mathbf{L}_p = \pm \frac{c\epsilon_0 E_0^2 a^3 t_p}{2d\omega} \hat{\mathbf{z}} \quad (1)$$

where \pm represents right and left circular polarizations of the laser, $\hat{\mathbf{z}}$ is the incident direction of the light, c , ϵ_0 , E_0 , t_p , d , ω and a are the speed of light, permeability, magnitude of electric field, pulse duration, thickness of the sample, angular frequency and lattice constant respectively. By using the experimental values from Ref. [4], we find the average angular momentum of the laser absorbed by one atom is about $10^{-4}\hbar$ per each laser pulse, assuming

that the angular momentum of the light is completely transferred to the electron orbitals and there is no relaxation during the process. Thus, the maximum angular momentum transferred from the light to the orbital moment is at least 2-3 orders of magnitude too small to account for the experimentally observed switching.

The second simple estimation is to consider the interaction of the light with a free electron. The classical equation of motion of the electron with the circularly polarized light is

$$m \frac{d^2 \mathbf{r}}{dt^2} = eE_0(\hat{\mathbf{x}} \cos \omega t \pm \hat{\mathbf{y}} \sin \omega t) \quad (2)$$

where E_0 is the magnitude of the electric field, and we consider the normal incident ($\hat{\mathbf{z}}$) of light on the film. The above equation yields an orbital angular momentum of the electron,

$$\delta \mathbf{L}_c \equiv m \mathbf{r} \times (d\mathbf{r}/dt) = \pm (eE_0)^2 / (m\omega^3) \hat{\mathbf{z}}. \quad (3)$$

By using the experimental values of E_0 and ω derived from Ref. [4], we find that $\delta \mathbf{L}_c$ is about $10^{-4} - 10^{-3} \hbar$ which is again 2-3 orders of magnitude too small to switch the magnetization. One might improve the estimation by replacing the free electron model with a bound electron which is subject to its internal resonant frequencies and damping parameters [16]. With reasonable material parameters, the order of magnitude remains about the same.

Motivated by the failure of the above simple estimation to explain the experimental results, we consider below the IFE for general bands by using the quantum description of the electron orbitals.

III. INDUCED ORBITAL MOMENT

We use the time-dependent perturbation theory to calculate the induced orbital momentum of an arbitrary band state whose wavefunction is denoted by $\psi_{n\mathbf{k}}^{(0)}(\mathbf{r})$ where n is the band index. The standard interaction between the circularly-polarized light and the electron is

$$V(t) = -eE_0 \left(x \cos(\omega t - \frac{\omega z}{c}) \pm y \sin(\omega t - \frac{\omega z}{c}) \right) [\theta(t) - \theta(t - t_p)] \quad (4)$$

where $\theta(t)$ is the step function, t_p is the laser pulse duration and x, y, z are three components of position operator (\mathbf{r}). The first order correction to the wavefunction by the above perturbation is

$$\psi_{n\mathbf{k}}(t) = e^{-i\omega_{n\mathbf{k}}t} \psi_{n\mathbf{k}}^{(0)} + \sum_{m\mathbf{k}' \neq n\mathbf{k}} c_{n\mathbf{k},m\mathbf{k}'}(t) e^{-i\omega_{m\mathbf{k}'}t} \psi_{m\mathbf{k}'}^{(0)} \quad (5)$$

where

$$c_{n\mathbf{k},m\mathbf{k}'}(t) = -\frac{i}{\hbar} \int_0^t dt' \int d^3\mathbf{r} \psi_{n\mathbf{k}}^{*(0)} V(t') \psi_{m\mathbf{k}'}^{(0)} e^{i\omega_{n\mathbf{k},m\mathbf{k}'} t'} \quad (6)$$

and $\omega_{n\mathbf{k},m\mathbf{k}'} = \omega_{n\mathbf{k}} - \omega_{m\mathbf{k}'}$.

The time-dependent average z-component orbital momentum $L_z \equiv xp_y - yp_x$ can be calculated by using the equation of motion,

$$\frac{d}{dt} \langle L_z \rangle_{n\mathbf{k}} = \langle \psi_{n\mathbf{k}}(t) | [L_z, V(t)] | \psi_{n\mathbf{k}}(t) \rangle \quad (7)$$

To proceed further, we explicitly use the Bloch states where $\psi_{n\mathbf{k}}^{(0)}(\mathbf{r}) = u_{n\mathbf{k}}(\mathbf{r}) \exp(i\mathbf{k} \cdot \mathbf{r})$ for calculating the matrix elements. The spatial integration in Eq. (6) can be carried out by separating the integration over a unit cell and summation over all periodic unit cells, i.e., replacing $\int d^3\mathbf{r}$ by $\sum_{\mathbf{R}_i} \int_{cell} d^3\mathbf{r}$, where \mathbf{R}_i is the lattice site. The summation over \mathbf{R}_i yields the crystal momentum conservation, $\mathbf{k}' = \mathbf{k} \pm (\omega/c)\hat{\mathbf{z}} + \mathbf{G}$, where \mathbf{G} is the reciprocal lattice vector. For the integration within a unit cell, we take the slowly varying function $\exp[i(\omega/c)z] \approx 1$. After explicitly carrying out spatial and time integration, we find,

$$\delta L_z = \pm \frac{4e^2 E_0^2}{\hbar} \sum_{n,m,\mathbf{k}} \left| \langle u_{n\mathbf{k}} | \frac{\partial u_{m\mathbf{k}'}}{\partial k'_x} \rangle \right|^2 \frac{\sin^2 [(\omega + \omega_{n\mathbf{k}} - \omega_{m\mathbf{k}'})t_p/2] (f_{n\mathbf{k}} - f_{m\mathbf{k}'})}{(\omega + \omega_{n\mathbf{k}} - \omega_{m\mathbf{k}'})^2 + 1/\tau^2}. \quad (8)$$

where $f_{m\mathbf{k}'}$ ($f_{n\mathbf{k}}$) are the Fermi distribution functions, $\mathbf{k}' = \mathbf{k} + (\omega/c)\hat{\mathbf{z}}$, and τ is a phenomenological parameter representing the energy relaxation time (further discussion follows).

Comparing the above equation to that of the standard transition probability between two atomic energy levels by the light, one finds several differences. First, the Fermi distribution function limits the transition between occupied and unoccupied states of the bands. Second, the momentum conservation $\mathbf{k}' = \mathbf{k} + (\omega/c)\hat{\mathbf{z}}$ implies that the difference between \mathbf{k}' and \mathbf{k} is small, thus the energy difference would be small as well if the transition occurs between the same band ($n = m$); i.e., $\omega_{n\mathbf{k}} - \omega_{n\mathbf{k}'} \ll \hbar\omega$. Therefore, the major contribution of the orbital momentum comes from the interband transition ($n \neq m$) with nearly same $\mathbf{k} \approx \mathbf{k}'$ and $\omega_{n\mathbf{k}} - \omega_{m\mathbf{k}} \approx \pm\omega$. Third, the lifetime τ of the excited states of the itinerant electrons is finite. Two essential contributions are impurity scattering and some other intrinsic scattering such as phonons and electron-electron interactions. A rough estimate of the relaxation time would be shorter than $\hbar/k_B T$ (where T is the temperature). If one takes the temperature at $T = 500$ K, τ would be no longer than 10^{-14} s. We will assume the relaxation time τ as a parameter which is included in Eq. (8). We point out, the resonant condition $\omega_{n\mathbf{k}} - \omega_{m\mathbf{k}'} = \omega$

in Eq. (8) would yield a singularly large contribution with an infinite relaxation time. The role of the finite relaxation is to broaden the spectrum of the states contributing to the induced orbital momentum.

IV. ESTIMATION OF INDUCED ORBITAL MOMENT

As an example of the application of Eq. (8), we consider the transition of the simplified band structure depicted in Fig. (1) where two hypothetical bands are separated by a band gap $\hbar\omega_0$ with each band characterized by bandwidth W_i ($i = 1, 2$). Both bands are parabolic. The matrix element in Eq. (8) depends on the details of the Bloch wavefunction. If we construct the Bloch state by a local atomic Wannier function $\phi_n(\mathbf{r})$

$$u_{n\mathbf{k}}(\mathbf{r}) = \frac{1}{\sqrt{N}} \sum_{\mathbf{R}} e^{-i\mathbf{k}\cdot(\mathbf{r}-\mathbf{R})} \phi_n(\mathbf{r} - \mathbf{R}) \quad (9)$$

where N is the number of sites in the system, we find

$$\langle u_{n\mathbf{k}} | \frac{\partial u_{m\mathbf{k}'}}{\partial k'_x} \rangle = \beta_{mn} + \sum_{\Delta} \gamma_{mn}(\Delta) \cos(\mathbf{k} \cdot \Delta) \quad (10)$$

where $\beta_{mn} = -\int d\mathbf{r} \phi_m^*(\mathbf{r}) x \phi_n(\mathbf{r})$ is the on-site dipolar matrix element, and $\gamma_{mn}(\Delta) = -\int d\mathbf{r} \phi_m^*(\mathbf{r} - \Delta) x \phi_n(\mathbf{r})$ is the overlap integration of the wavefunctions between nearest neighbor atomic site Δ . In general, $|\beta_{mn}| \gg |\gamma_{mn}|$ if the Wannier orbital of ϕ_n and ϕ_m do not have same spatial symmetry which would make β_{mn} identically zero (known as the selection rule), and thus the matrix element would be weakly dependent on \mathbf{k} and we simply take it as a constant. With the above simplifications, Eq. (8) now reduces to,

$$\delta L_z = \pm C \left(\frac{a^2 \omega^2}{4\pi^3} \right) \int_0^{\epsilon_F} d\epsilon g(\epsilon) \frac{\sin^2[(\omega - \omega_0 - \alpha\epsilon)t_p/2]}{(\omega - \omega_0 - \alpha\epsilon)^2 + 1/\tau^2} \equiv \pm CI \quad (11)$$

where $C = 2e^2 E_0^2 a^2 / (\hbar \omega^2)$, $g(\epsilon)$ is the density of states, $\alpha = (1 + W_2/W_1)/\hbar$, and the last equality defines the dimensionless quantity I to be numerically calculated.

To access the dependence of δL_z on the parameters entering in Eq. (11), we numerically compute I for various plausible parameters relevant to the experimental materials. In Fig. (2), we show the influence of the (or the energy gap $\hbar\omega_0$) between occupied and unoccupied band. Clearly, the maximum values occurs when $\omega - \omega_0$ is near the vicinity of ϵ_F . More importantly, both the peak value and the peak width depend on the relaxation time. As we discussed earlier, the relaxation time limits the overall non-equilibrium orbital

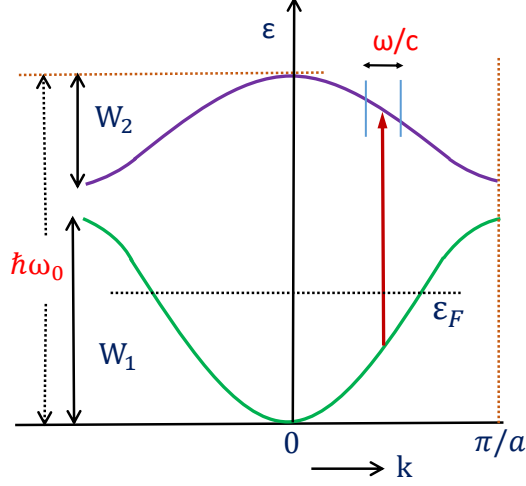


FIG. 1: (color online) Laser induced transition between two hypothetical bands where ϵ_F represents Fermi energy and W_1 , W_2 are the band width of lower and upper band respectively. The red arrows indicates the transition from the lower band at a particular k state to the upper band at $k' - k \approx \omega/c$.

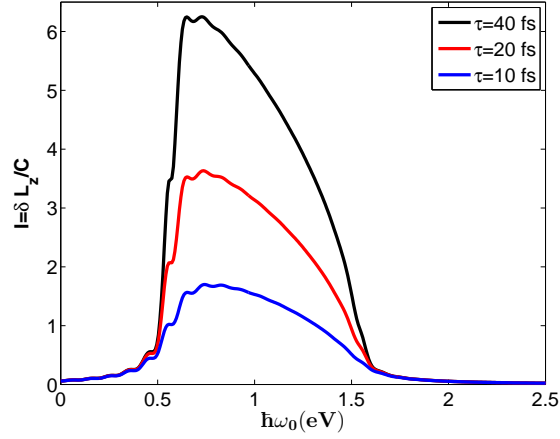


FIG. 2: (color online) The induced orbital momentum as a function of the band separation $\hbar\omega_0$ for three different relaxation times. The other parameters are $t_p = 50$ (fs) and $\alpha = 1.5$ eV/ \hbar .

momentum: the laser induced excitations from the occupied states to the unoccupied states has been balanced by the relaxation processes. Another important parameter is the laser pulse duration t_p . In Fig. (3), we show the peak values derived from Fig. 2 as a function of the pulse width. At a small t_p , the orbital momentum linearly increases with the pulse duration, and it saturates at a certain value, typically of the order of a few tens of fs.

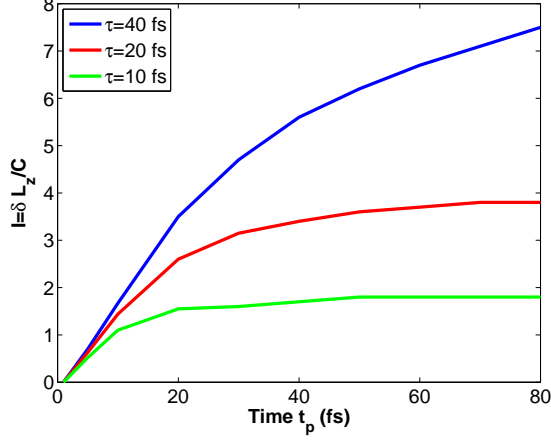


FIG. 3: (color online) The induced orbital momentum as a function of laser pulse duration t_p for $\alpha = 1.5$ (eV/ \hbar).

V. DISCUSSIONS

We have calculated the laser induced orbital momentum for generic band structure. In experimental systems, band structures are far more complicated. We argue here that our simplified treatments of the band structure capture the essential features of the laser driven processes: since the most important factor for the magnitude of the orbital momentum is the relaxation time as we have seen in Fig. (2) and (3), the relaxation process is effectively washed out the detail dispersion relation of the band. We have assumed a minimum relaxation rate in our estimation, the results obtained here is an overestimate of the laser induced momentum.

It is interesting to compare the magnitude of the induced orbital momentum calculated here with two earlier estimations based on the classical free electron model, Eq. (3), and the total angular momentum transfer model, Eq. (1). The relative ratios are

$$\frac{\delta L_z}{\delta L^c} = 2 \frac{ma^2\omega}{\hbar} I$$

and

$$\frac{\delta L_z}{\delta L_p} = 4 \left(\frac{d}{a} \right) \left(\frac{e^2}{c\epsilon_0 a t_p \hbar \omega} \right) I$$

By using the experimental values [4, 9], all three estimates yield an angular momentum that are roughly same orders of magnitude, i.e., about $\delta L_z \approx 10^{-4} - 10^{-3} \hbar$ per atom. We note that a recently published article [17] claimed that theoretical estimation yields a reasonable magnitude to explain the above experiment; this error was due to mis-identification of

the experimental value [18]. Thus, the IFE is unlikely to be a dominant origin for the experimentally observed laser polarization dependent magnetization switching.

Finally, we wish to comment on the possible mechanisms of the experimentally observed switching. Since the spatial coverage of the laser field is usually of the order of several micrometers, the magnetization distribution would be highly non-uniform. Upon laser radiation, both heat and magnetization have spatial dependence. In a macroscopic sized film, the non-uniform distribution in turn leads to a strong and complicated dipolar interactions that govern the magnetization dynamics and switching [19]. In the earlier experiments, one can even observe the magnetization switching with an unpolarized laser beam and without any magnetic field [6]; a result indicates the role of the non-uniform distribution in the symmetry-breaking processes. For the observed helix dependent switching, the IFE alone is not sufficient, and most likely, the extrinsic effects such as domain wall structure and pinning play a key role. Such speculations seem consistent with a subtle dependence of switching on a narrow range of a larger pulse width, film compositions, and the number of repeated laser pulses [20].

VI. CONCLUSION AND ACKNOWLEDGMENT

We have shown by using the time-dependent quantum perturbation theory for generic itinerant bands that, the inverse Friday effect, or the polarized light induced orbital momentum is too small to account for the observed magnetization switching. The calculated magnitude is comparable to those estimated from simple free electron model and from the maximum angular momentum of the laser beam to the electrons. This work was supported by NSF (ECCS-1404542).

-
- [1] I. Radu, K. Vahaplar, C. Stamm, T. Kachel, N. Pontius, H. A. Durr, T. A. Ostler, J. Barker, R. F. L. Evans, R. W. Chantrell, A. Tsukamoto, A. Itoh, A. Kirilyuk, Th Rasing, and A. V. Kimel. Transient ferromagnetic-like state mediating ultrafast reversal of antiferromagnetically coupled spins. *Nature*, 472(7342):205–208, Apr 2011.
 - [2] C. D. Stanciu, F. Hansteen, A. V. Kimel, A. Kirilyuk, A. Tsukamoto, A. Itoh, and Th. Rasing. All-optical magnetic recording with circularly polarized light. *Phys. Rev. Lett.*, 99:047601, Jul

2007.

- [3] Sabine Alebrand, Matthias Gottwald, Michel Hehn, Daniel Steil, Mirko Cinchetti, Daniel Lacour, Eric E. Fullerton, Martin Aeschlimann, and Stphane Mangin. Light-induced magnetization reversal of high-anisotropy tbco alloy films. *Applied Physics Letters*, 101(16), 2012.
- [4] S. Mangin, M. Gottwald, C-H. Lambert, D. Steil, V. Uhl, L. Pang, M. Hehn, S. Alebrand, M. Cinchetti, G. Malinowski, Y. Fainman, M. Aeschlimann, and E. E. Fullerton. Engineered materials for all-optical helicity-dependent magnetic switching. *Nat Mater*, 13, Mar 2014.
- [5] E. Beaurepaire, J.-C. Merle, A. Daunois, and J.-Y. Bigot. Ultrafast spin dynamics in ferromagnetic nickel. *Phys. Rev. Lett.*, 76:4250–4253, May 1996.
- [6] T. A. Ostler, J. Barker, R. F. L. Evans, R. W. Chantrell, U. Atxitia, O. Chubykalo-Fesenko, S. El Moussaoui, L. Le Guyader, E. Mengotti, L. J. Heyderman, F. Nolting, A. Tsukamoto, A. Itoh, D. Afanasiev, B. A. Ivanov, A. M. Kalashnikova, K. Vahaplar, J. Mentink, A. Kirilyuk, Th Rasing, and A. V. Kimel. Ultrafast heating as a sufficient stimulus for magnetization reversal in a ferrimagnet. *Nature Communications*, 3:666 EP –, Feb 2012. Article.
- [7] U. Atxitia, T. Ostler, J. Barker, R. F. L. Evans, R. W. Chantrell, and O. Chubykalo-Fesenko. Ultrafast dynamical path for the switching of a ferrimagnet after femtosecond heating. *Phys. Rev. B*, 87:224417, Jun 2013.
- [8] Xiankai Jiao, Lei Xu, and Shufeng Zhang. Self-consistent bloch equation for modeling element-specific demagnetization of magnetic alloys and multilayers. *Journal of Applied Physics*, 117(19):193901, 2015.
- [9] K. Vahaplar, A. M. Kalashnikova, A. V. Kimel, S. Gerlach, D. Hinzke, U. Nowak, R. Chantrell, A. Tsukamoto, A. Itoh, A. Kirilyuk, and Th. Rasing. All-optical magnetization reversal by circularly polarized laser pulses: Experiment and multiscale modeling. *Phys. Rev. B*, 85:104402, Mar 2012.
- [10] Andrei Kirilyuk, Alexey V. Kimel, and Theo Rasing. Ultrafast optical manipulation of magnetic order. *Rev. Mod. Phys.*, 82:2731–2784, Sep 2010.
- [11] P. Nieves and O. Chubykalo-Fesenko. Modeling of ultrafast heat- and field-assisted magnetization dynamics in fept. *Phys. Rev. Applied*, 5:014006, Jan 2016.
- [12] J. Deschamps, M. Fitaire, and M. Lagoutte. Inverse faraday effect in a plasma. *Phys. Rev. Lett.*, 25:1330–1332, Nov 1970.
- [13] Riccardo Hertel. Theory of the inverse faraday effect in metals. *Journal of Magnetism and*

- Magnetic Materials*, 303(1):L1 – L4, 2006.
- [14] J. P. van der Ziel, P. S. Pershan, and L. D. Malmstrom. Optically-induced magnetization resulting from the inverse faraday effect. *Phys. Rev. Lett.*, 15:190–193, Aug 1965.
 - [15] M. Battiato, G. Barbalinardo, and P. M. Oppeneer. Quantum theory of the inverse faraday effect. *Phys. Rev. B*, 89:014413, Jan 2014.
 - [16] B. A. Zon and V. Y. Kupershmidt. Inverse Faraday effect and the radiation shift of the cyclotron frequency in a gas of free electrons. *Radiophysics and Quantum Electronics*, 19:1072–1076, October 1976.
 - [17] Xiang-Jun Chen. Fundamental mechanism for all-optical helicity-dependent switching of magnetization. *Scientific Reports*, 7:41294 EP –, Jan 2017. Article.
 - [18] The author of Ref. [17] erranously quoted the laser intensity within the pulse width to be 500 mJ/s cm² which is two orders of magnitude more than the experimental values.
 - [19] L. Gierster, A.A. nal, L. Pape, F. Radu, and F. Kronast. Laser induced magnetization switching in a tbfec ferrimagnetic thin film: discerning the impact of dipolar fields, laser heating and laser helicity by {XPEEM}. *Ultramicroscopy*, 159, Part 3:508 – 512, 2015. Special Issue: LEEM-PEEM 9.
 - [20] Eric E. Fullerton, Private communication.